Electron scattering from perfluorocyclobutane (c-C_4F_8)

M. Jelisavcic and R. Panajotovic
Atomic and Molecular Physics Laboratories, Research School of Physical Sciences & Engineering, Australian National University, Canberra Australian Capital Territory, Australia

M. Kitajima, M. Hoshino, and H. Tanaka
Physics Department, Sophia University, Chiyoda-ku, Tokyo, Japan

S. J. Buckman[a)]
Atomic and Molecular Physics Laboratories, Research School of Physical Sciences & Engineering, Australian National University, Canberra Australian Capital Territory, Australia

(Received 12 May 2004; accepted 21 June 2004)

We report experimental results for electron scattering from perfluorocyclobutane, c-C_4F_8, obtained from measurements in our two laboratories. A set of differential, integral, and momentum transfer cross sections is provided for elastic scattering for incident electron energies from 1.5 to 100 eV. Inelastic scattering (vibrational excitation) cross sections have been measured for incident electron energies of 1.5, 2, 5, 6, and 7 eV. In order to investigate the role of intermediate negative ions (resonances) in the scattering process we have also measured an excitation function for elastic scattering and vibrational excitation of the ground electronic state of C_4F_8 for incident energies between 0.6 and 20 eV. These results are compared with the limited amount of data available in the literature for scattering from this molecule. © *2004 American Institute of Physics.*
[DOI: 10.1063/1.1782174]

I. INTRODUCTION

Perfluorocyclobutane (c-C_4F_8) is a very common processing gas in the plasma etching of silicon dioxide, which is an important step in the manufacture of semiconductor microelectronics. A particular advantage of this gas is the good selectivity it offers in the etching of silicon dioxide over silicon.[1] However, little is known of the magnitude of the electron scattering and excitation processes for this gas. In addition, because of its extensive use in plasma etching, c-C_4F_8 is of environmental interest because it is a global warming gas.[2] In order to understand the complex chemical processes in the upper atmosphere, and the role that electron driven processes may play in determining the global warming capacity of C_4F_8, an understanding of the cross sections for low-energy electron collision processes is important.[3] Despite the need for fundamental scattering information, there have been just a few experimental and theoretical studies regarding electron impact cross sections for scattering from c-C_4F_8.

Some years ago Ishii *et al.*[4] measured electron transmission spectra of c-C_4F_8 and noticed a resonant feature just above zero electron energy. This is broadly consistent with the positive electron affinity of 0.63 eV measured in an electron attachment experiment by Miller *et al.*[5] Ishii *et al.* also measured the energies of the low-lying σ^* resonances in other normal and cyclic perfluoroalkanes and calculated negative ion energies in both the alkanes and their perfluro derivatives. Amongst other things, they concluded that the negative ion energies of the perfluoro-*n*-alkanes decreased markedly as the size of the molecule increased and that the ground state anions of the cyclic perfluoroalkanes are more stable than that of the corresponding normal perfluoroalkanes. Total cross sections for c-C_4F_8 have been measured recently by Sanabia *et al.*,[6] in the low-energy (1–20 eV) range, and by Nishimura *et al.*[7] at energies from 2 to 3000 eV. Sanabia *et al.* suggested the existence of Ramsauer-Townsend minimum at an energy near 3.5 eV.

There have been several measurements of the electron attachment cross section for c-C_4F_8 (Kurepa *et al.*,[8] Spyrou *et al.*,[9] Chutjian *et al.*,[10] and Novak *et al.*[11]). All of these measurements indicated that there are two primary attachment mechanisms. At energies above 1 eV, the dominant process is dissociative attachment forming F^-, and at lower energies, the parent negative ion $C_4F_8^-$ is formed. Swarm parameters such as electron drift velocity, ionization, and attachment coefficients were measured by Novak *et al.*,[11] Naidu *et al.*,[12] and Yamaji *et al.*[13] There have been two measurements of partial ionization cross section performed by Toyoda *et al.*[14] and Jiao *et al.*[15] and there are substantial differences between these two sets of results, depending on the particular positive ion fragment involved. For all of these processes, recommended cross sections have been proposed in a comprehensive and recent review paper by Christophorou and Olthoff.[3] Also, a cross section "set" has been proposed by Font *et al.*[16] for the simulation of c-C_4F_8 plasma discharges. They used the theoretical calculations of Winstead and McKoy[17] for the elastic and electronic excitation cross sections, and a vibrational cross section based on the Born approximation. The latter was determined by a Boltzmann analysis to the available swarm-derived transport parameters.

a)Author to whom correspondence should be addressed. Electronic mail: stephen.buckman@anu.edu.au

TABLE I. Absolute differential cross sections in units of 10^{-16} cm^2 sr^{-1}, for elastic electron scattering from C_4F_8. The ANU results are designated (*A*) and the Sophia results (*S*). For the ANU results the figures in parentheses represent the absolute error, expressed as a percentage, while for the Sophia data the estimated uncertainty is ±15%. The figures at the base of each column are the integral elastic and elastic momentum transfer cross sections, for which the estimated uncertainties are 20%–25%.

Angle (deg)	ENERGY (eV)					
	1.5 (*A*)	1.5 (*S*)	2.0 (*A*)	2.0 (*S*)	2.6 (*S*)	3.0 (*S*)
20	0.604(46)	1.534	1.266(39)	1.413	1.424	1.802
30	1.816(24)	1.623	0.823(17)	2.020	2.712	2.977
40	2.083(24)	2.455	2.511(17)	3.077	3.594	3.516
50	2.669(11)	2.705	3.682(9)	3.638	4.061	3.951
60	2.528(9)	2.838	2.668(7)	3.149	3.378	2.889
70	2.288(7)	2.398	2.021(7)	2.694	1.963	1.522
80	1.575(7)	2.009	1.238(7)	1.574	1.194	0.821
90	1.105(7)	1.338	0.662(7)	0.909	0.556	0.414
100	0.700(7)	0.914	0.365(7)	0.559	0.332	0.397
110	0.510(7)	0.642	0.295(8)	0.410	0.378	0.684
120	0.477(7)	0.593	0.389(7)	0.466	0.613	0.941
130	0.571(7)	0.693	0.605(6)	0.708	0.905	1.213
ICS	16.9	18.8	16.8	18.5	18.1	18.7
MTCS	12.5	14.0	10.8	12.1	11.0	12.9
Angle (deg)	4.0 (*S*)	5.0 (*A*)	5.0 (*S*)	6.0 (*A*)	7.0 (*A*)	8.0 (*S*)
15				8.451(36)		
20	3.050	5.870(8)	5.703	8.305(8)	11.574(8)	12.021
30	3.704	4.769(7)	4.480	6.891(7)	8.000(7)	9.142
40	4.011	3.893(7)	3.947	4.669(7)	4.783(7)	4.826
50	3.293	2.342(8)	2.454	2.679(7)	2.273(7)	2.068
60	2.137	1.025(8)	1.212	1.146(7)	0.983(7)	0.995
70	0.960	0.600(7)	0.701	0.829(6)	0.844(7)	1.344
80	0.525	0.676(7)	0.803	0.920(6)	1.032(6)	1.511
90	0.691	0.906(8)	0.936	1.020(6)	1.048(7)	1.542
100	0.949	1.032(8)	1.111	0.966(7)	0.913(8)	1.218
110	1.248	1.027(8)	1.301	0.883(7)	0.810(7)	1.267
120	1.580	1.030(7)	1.182	0.879(8)	0.808(7)	1.262
130	1.769	1.110(6)	1.311	0.948(6)	0.919(7)	1.430
ICS	21.4	22.5	21.3	22.8	24.9	30.5
MTCS	16.6	14.2	16.2	11.9	13.3	18.5
Angle (deg)	10 (*A*)	10 (*S*)	15 (*A*)	15 (*S*)	20 (*A*)	20 (*S*)
10			37.581(35)		47.398(7)	
15						
20	15.486(13)	15.035	15.553(8)	15.908	15.956(7)	17.773
30	8.782(12)	9.273	5.632(8)	6.280	2.880(7)	3.890
40	3.465(12)	4.004	1.299(8)	1.568	0.990(7)	1.160
50	1.330(8)	1.344	1.166(8)	1.279	1.812(6)	2.448
60	1.360(6)	1.428	1.834(6)	2.045	2.016(8)	2.776
70	1.840(6)	1.980	1.961(7)	2.663	1.725(7)	2.390
80	1.885(7)	1.989	1.848(6)	2.290	1.452(7)	1.929
90	1.558(6)	1.796	1.687(6)	2.112	1.167(7)	1.595
100	1.316(7)	1.799	1.401(6)	1.865	1.020(6)	1.376
110	1.295(7)	1.630	1.266(6)	1.758	1.088(7)	1.381
120	1.363(8)	1.711	1.309(6)	1.600	1.302(7)	1.599
130	1.540(7)	2.108	1.621(7)	2.022	1.780(7)	2.117
ICS	34.9	35.6	34.2	35.2	32.9	37.8
MTCS	21.5	22.3	19.0	21.6	17.2	20.4

TABLE I. (*Continued*.)

Angle (deg)	30 (*S*)	60 (*S*)	100 (*S*)
20	14.627	5.112	3.822
30	1.554	3.479	3.045
40	2.500	2.142	1.557
50	2.530	1.403	0.769
60	1.890	0.842	0.538
70	1.543	0.616	0.489
80	1.073	0.423	0.275
90	0.827	0.363	0.200
100	0.921	0.352	0.244
110	0.872	0.472	0.300
120	1.270	0.666	0.373
130	1.700	0.935	0.674
ICS	31.3	16.1	11.0
MTCS	15.6	6.21	3.68

The calculation of Winstead and McKoy[17] is the only available theoretical calculation of differential or integral cross sections for low energy electron scattering from c-C_4F_8. They used the Schwinger multichannel method (SMC), within the static exchange approximation–polarization effects were not included. Resonance structures observed in integral cross section were analyzed in terms of temporary electron trapping in virtual valence orbitals. As c-C_4F_8 possesses a large dipole polarizability (>50 a.u.), it may be expected that the noninclusion of polarization effects will have important ramifications for predicting the low-energy scattering cross sections.

In light of the above it would appear that the available data on electron scattering cross sections from c-C_4F_8 are still incomplete. In particular, momentum transfer and integral elastic scattering cross sections, as well as differential cross sections for elastic and vibrational excitation are required. The main aim of this work is to provide a complete set of absolute differential, integral, and momentum transfer cross sections for elastic electron scattering and vibrational excitation of the ground electronic state of c-C_4F_8. Absolute elastic and vibrational excitation differential cross sections for electron scattering from c-C_4F_8 were measured at a number of energies between 1.5 and 100 eV for elastic and 1.5 and 7 eV for vibrational excitation and for scattering angles between 20°–130°. Integral and momentum transfer cross sections were derived from differential cross sections by extrapolating results to 0° and 180°, and integrating the resultant cross section.

II. EXPERIMENTAL DETAILS

The experimental work described here was performed in two laboratories: the Australian National University (ANU) and Sophia University (SU). A full description of the apparatus used in both laboratories has been given in previous publications,[18–20] so we will only discuss the relevant aspects important for this work.

The overall operation of the two spectrometers is very similar, with both capable of producing low-energy electron beams with reasonable energy resolution (50 meV for the ANU spectrometer and 30 meV for the SU spectrometer). The absolute value of the incident energy was determined through calibration against the positions of well known resonances observed in electron-atom/molecule collision processes. For higher incident electron energies (>10 eV) energy calibration was made against the low-lying $1s2s^2\,{}^2S$ resonance in He, and for low incident electron energies (<10 eV) calibration was made against $^2\Sigma_g$ resonance in N_2^-. In both laboratories, the relative flow technique[21,22] is the method of choice for putting measured scattering intensities on an absolute scale. The technique involves the measurements of relative electron scattering intensities for the gas under the study (c-C_4F_8) and for a so called standard gas, for which scattering cross sections are well known. In our measurements the standard gas was helium, because it is widely accepted that the elastic differential scattering cross sections for helium are very well known at incident energies below 50 eV.[23–25] The driving pressures for both gases are determined in such a way that the collisional mean-free-path for both gases is the same. Typical driving pressure used at ANU were 0.25 Torr (c-C_4F_8) and 1 Torr (He) while at SU the pressures were in the same proportion but approximately five times higher.

Both spectrometers can operate in two different data collection modes. In one, the angular dependence of scattering signal is measured at fixed impact energy and energy loss (differential cross section or DCS operational mode), while in the other, the energy loss and scattering angle are fixed but the incident energy is varied [excitation functions (EF) operational mode]. The absolute uncertainties on the measured cross sections are typically less then 10%–15% for elastic scattering and around 15% for vibrational excitation.

III. RESULTS AND DISCUSSION

A. Elastic scattering

Absolute differential cross sections for elastic scattering from c-C_4F_8 molecules at energies between 1.5 and 100 eV are presented in Table I. A comparison between the present results from both laboratories and the theoretical calculations of Winstead and McKoy[17] is provided in Figs. 1 and 2. In general, the level of agreement between the two sets of ex-

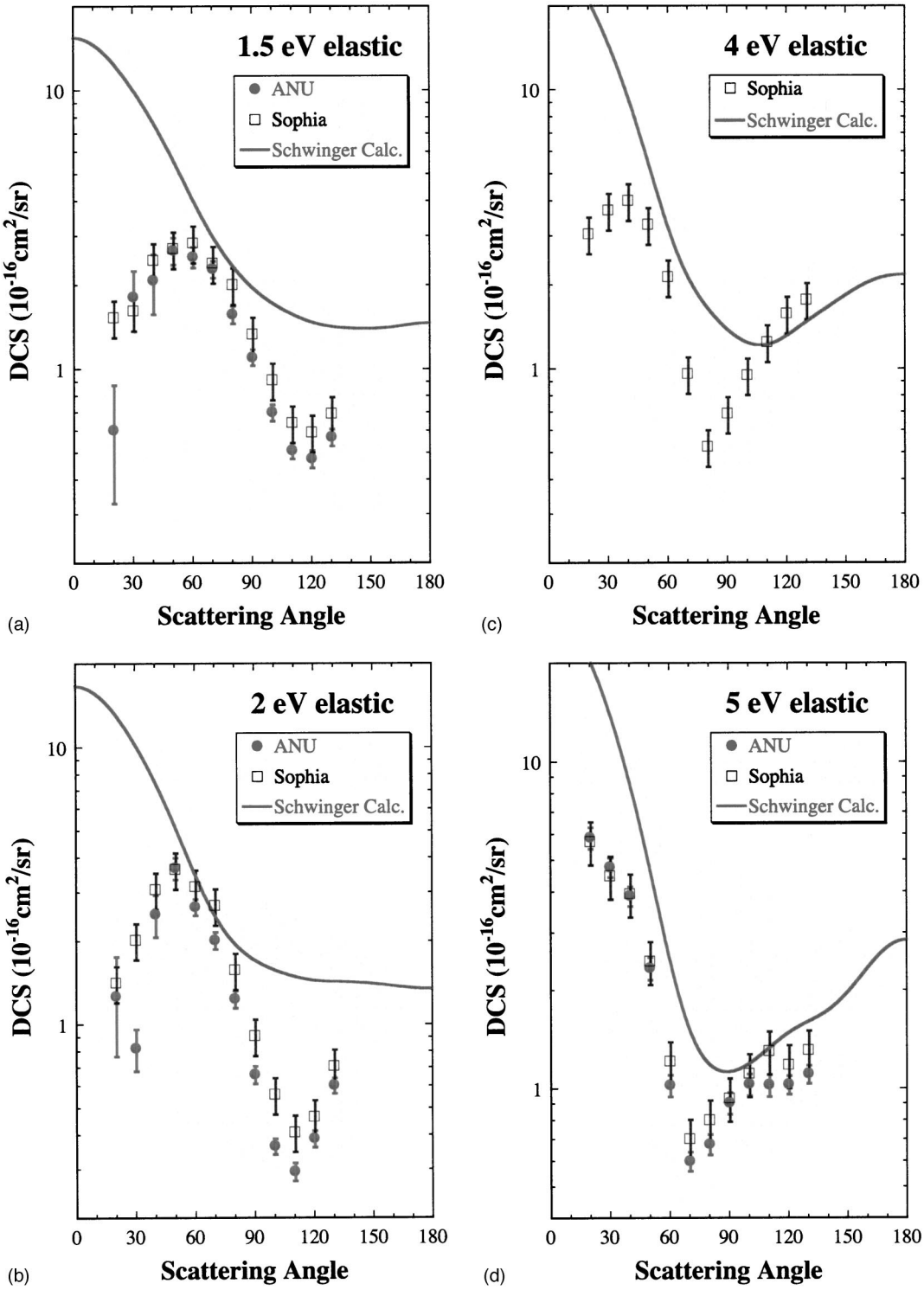

FIG. 1. Absolute differential cross sections for elastic electron scattering from C_4F_8 (in units of 10^{-16} cm^2 sr^{-1}) at (a) 1.5 eV, (b) 2.0 eV, (c) 4.0 eV, and (d) 5.0 eV. Present results: (●) ANU and (□) Sophia; (——) Schwinger variational calculation.[17]

perimental data from our two spectrometers is very good, while the level of agreement with the theoretical calculation varies markedly with energy, as discussed below.

In Fig. 1 we show the angular differential cross sections (DCS) at incident energies below 5 eV. It is evident that the shape of the DCS changes significantly for energies between 1.5 and 5 eV. At low energies, 1.5 and 2 eV [Figs. 1(a) and 1(b), respectively], the cross section decreases in magnitude towards forward angles, has a maximum of $\sim 3 \times 10^{-16}$ cm^2/sr at a scattering angle 60°, and a shallow minimum at around 120°. However, by 4 eV [Fig. 1(c)] the DCS has developed a sharper minimum at ~80° and the extent of forward scattering has increased. By 5 eV [Fig. 1(d)], the decreasing DCS at forward angles has changed to a rather more forward-peaked shape, consistent with the large dipole polarizability of this molecule, and the minimum in the cross

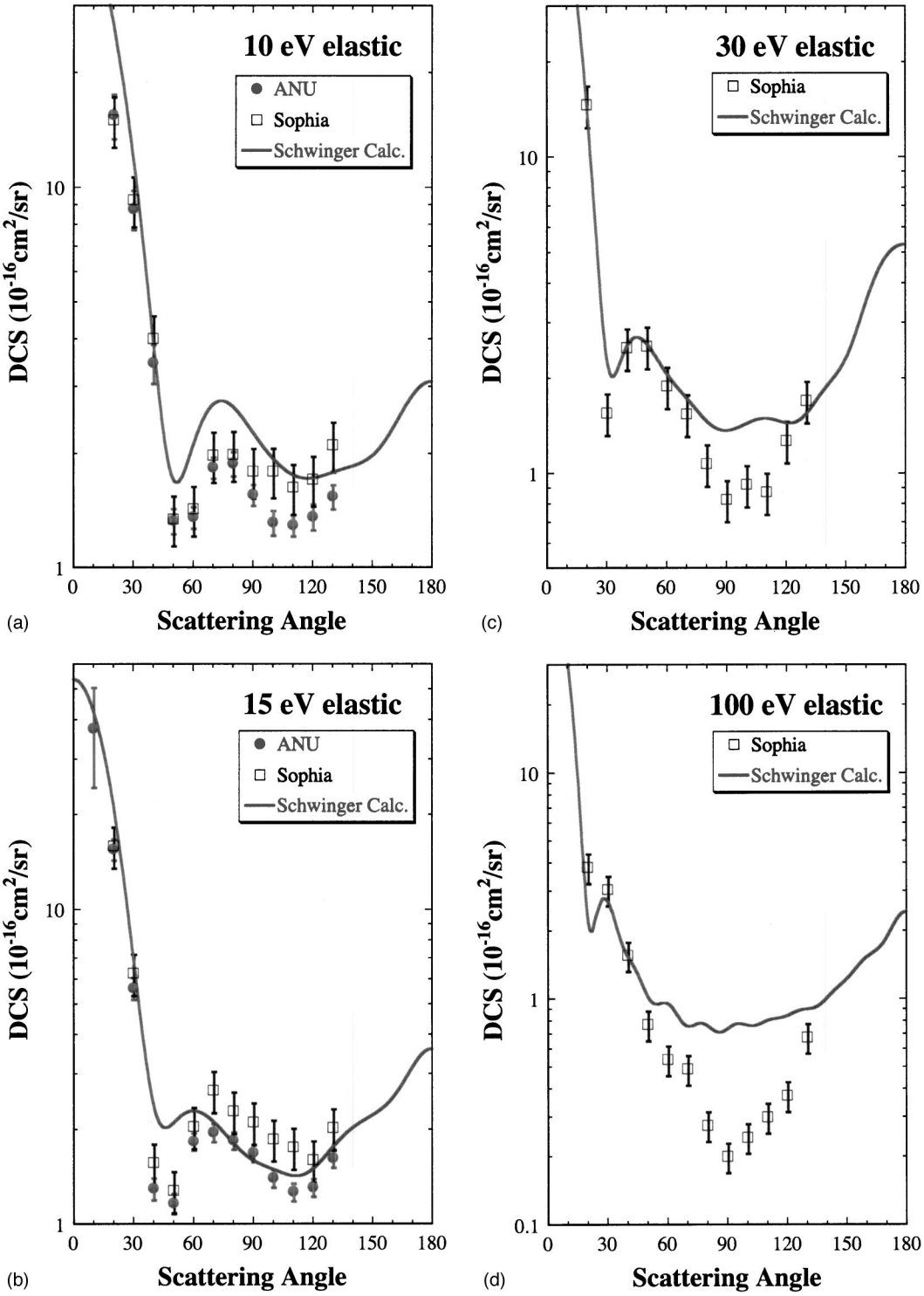

FIG. 2. Absolute differential cross sections for elastic electron scattering from C_4F_8 (in units of 10^{-16} cm^2 sr^{-1}) at (a) 10 eV, (b) 15 eV, (c) 20 eV, and (d) 100 eV. Present results: (●) ANU and (□) Sophia; (——) Schwinger variational calculation.[17]

section occurs at about 70°. At all of these energies the agreement between the two measurements is excellent. The same cannot be concluded for the level of agreement with the Schwinger multichannel calculation, which is also illustrated at all of these energies. At low energies (1.5 and 2 eV) it bears little resemblance to the experimental DCS in either shape or magnitude. However, by 5 eV the agreement in both shape and magnitude has improved considerably with the exception of the forward angle region where the theory still apparently overestimates the DCS.

At higher energies (Fig. 2) the DCS takes on more characteristic features—strong forward scattering is evident and some large angle diffraction effects are observed. Once again we see good agreement between the two experimental results and substantially better agreement between experiment and theory. At 10 and 15 eV [Figs. 2(a) and 2(b)] the theoretical

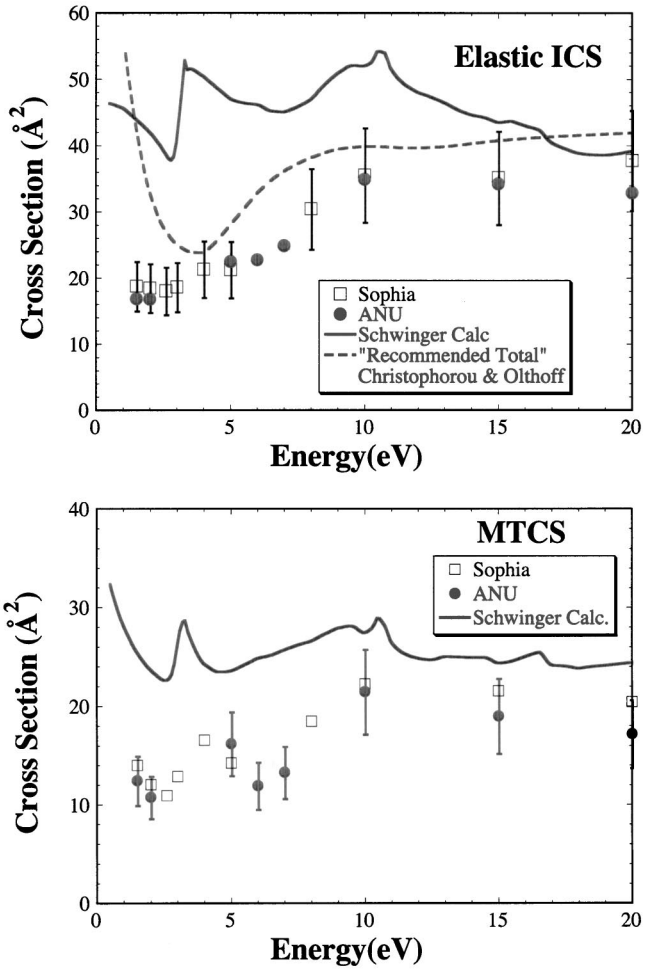

FIG. 3. (a) Integral elastic and (b) elastic momentum transfer cross sections for C_4F_8. Present results: (●) ANU and (□) Sophia; (——) Schwinger variational calculation;[17] (— — —) recommended total cross section.[3]

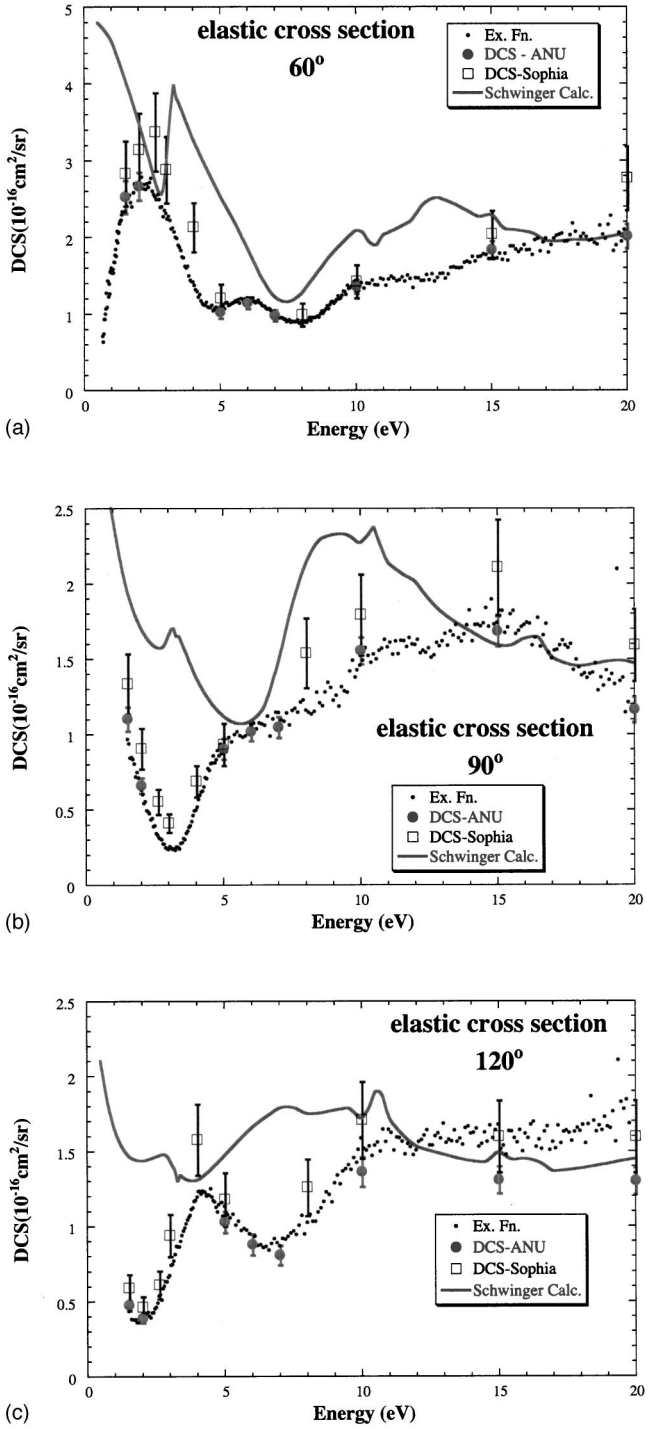

FIG. 4. Excitation functions for elastic scattering from C_4F_8 at scattering angles of (a) 60°, (b) 90°, and (c) 120°.

calculation reproduces all of the features of the experimental DCS, including a sharp but shallow minimum at ~50°, and is in excellent agreement with the magnitude of the measured cross section. At 30 and 100 eV [Figs. 2(c) and 2(d)] there is also good agreement between the Sophia results and the theory, particularly at forward and backward angles, but some differences in magnitude exist in the midangle region. Unfortunately the experimental results do not extend to angles lower than 20°, where the theoretical DCS is shown to increase enormously, which again is consistent with the large dipole polarizabilty of C_4F_8.

The differential elastic cross sections have been analyzed using a molecular phase shift approach,[26] in order to extrapolate the DCS to forward and backward angles and facilitate the derivation of elastic integral and momentum transfer cross sections. The cross section values are indicated at the foot of each column in Table I and the integral elastic cross section (ICS) and elastic momentum transfer cross section (MTCS) are shown in Figs. 3(a) and 3(b), respectively. The discrepancy between the experimental results and theoretical calculations at low energies is clearly reflected in the comparison of calculated ICS and MTCS, and values derived from the present DCS measurements. In both cases the theory is considerably larger in magnitude at energies below 10 eV. For the ICS we also compare the present results with the recommended total cross section of Christophorou and Olthoff[3] and note that the latter is larger at all energies than the present cross section, as expected. This is not the case for the theoretical elastic ICS, which is larger in magnitude than the total cross section for energies below 15 eV. As Winstead and McKoy suggested in their paper, this disagreement at low energies is most likely due to the enhancement of low energy *s*-wave scattering, and upward shift in the resonance energies, which are both artifacts introduced by using the static exchange approximation.

In order to investigate the negative ion resonances predicted by the theoretical calculations of Winstead and McKoy in the energy range 0 to 20 eV, measurements of the energy dependence (excitation functions or EF) of the elastic cross section were performed at three scattering angles 60°, 90°, and 120°. These are shown in Fig. 4, together with the ANU and SU DCS data at several fixed incident energies and the theoretical calculations. From Fig. 4 we can see that the shape of the excitation functions changes considerably with scattering angle. At a scattering angle of 60°, the EF has a pronounced peak at 2 eV which most likely corresponds to the resonance of symmetry $^2B_2$, predicted by the theory to lie at ~3 eV. Another feature is evident at ~6 eV and may correspond to an ^2E resonance predicted by the theoretical calculations at an energy of 8.1 eV, respectively. The higher energy reaches of the spectrum are reasonably flat and devoid of structure, although there may be a weak, broad feature centered at around 10 eV. The overall agreement between the theoretical calculations and our experimental results is reasonable if one assumes that the features in the theoretical EF are generally shifted to higher energies. However, as the theoretical calculations were made in the static exchange approximation, with no polarization effects included, resonance positions are shifted in energy by typically 2 to 4 eV.

At a scattering angle of 90°, the shape of the excitation function has changed significantly. At ~3 eV a deep minimum is observed, indicating perhaps the dominance of *p*-wave scattering in the scattering process at this energy. Other possible but very weak and broad resonance structures appear at energies of ~5, 11, and 15 eV.

Finally at a scattering angle of 120°, a strong resonant peak at 4 eV is clearly visible. This structure may be allied to those previously confirmed in dissociative attachment experiments (see Refs. 13 and 17 for a summary) and in the calculations of Winstead *et al.*[17] The latter indicate that this may be due to a resonance in the $^2A_1$ symmetry. At higher energies, 10–20 eV, the excitation function is reasonably flat and featureless at this scattering angle.

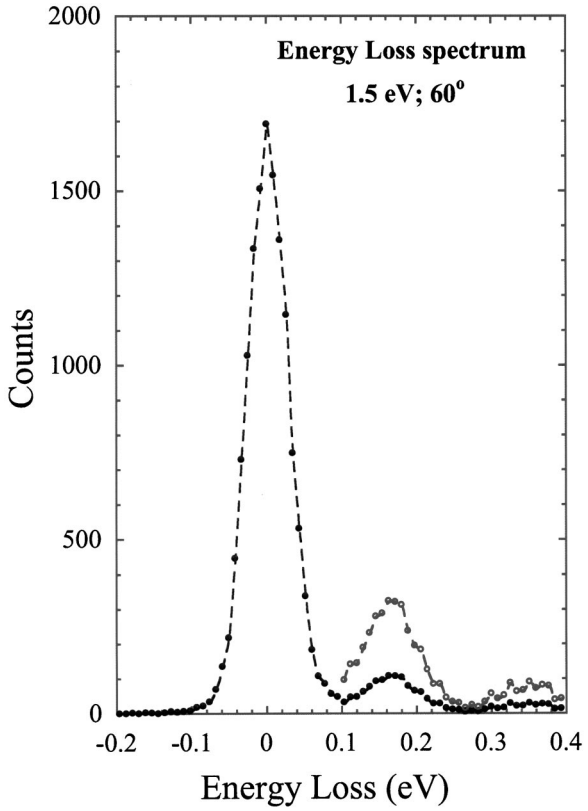

FIG. 5. Energy loss spectrum for C_4F_8 at an incident energy of 1.5 eV and a scattering angle of 60°.

B. Vibrational excitation

The vibrational energies of the fundamental modes of perfluorocyclobutane are not well documented. However, as C_4F_8 has the same symmetry as C_4H_8, one might expect the same vibrational modes as in the hydrocarbon analog but with significantly different (smaller) oscillation frequencies. Of the 25 possible modes of oscillation it would appear that only a few are strongly active in the gas phase.[27] For C_4F_8, an energy loss spectrum for electrons of 1.5 eV incident energy, which have been scattered through an angle of 60° is

TABLE II. Absolute differential cross sections in units of 10^{-16} cm^2 sr^{-1}, for vibrational excitation of C_4F_8. The figures in parentheses represent the absolute error, expressed as a percentage.

	Energy (eV)				
Angle (deg)	1.5	2	5	6	7
20	0.186(54)	0.808(65)	0.397(14)	0.417(12)	0.444(12)
30	0.485(12)	0.168(49)	0.183(12)	0.233(12)	0.269(12)
40	0.315(13)	0.211(18)	0.131(12)	0.175(13)	0.217(13)
50	0.218(13)	0.176(20)	0.115(12)	0.166(12)	0.202(12)
60	0.130(13)	0.100(12)	0.130(17)	0.161(12)	0.198(12)
70	0.094(13)	0.081(13)	0.136(17)	0.163(12)	0.192(12)
80	0.080(14)	0.074(12)	0.137(16)	0.159(13)	0.187(12)
90	0.077(16)	0.062(13)	0.137(17)	0.158(13)	0.185(12)
100	0.072(15)	0.062(13)	0.140(19)	0.160(14)	0.186(13)
110	0.072(14)	0.059(12)	0.136(17)	0.163(15)	0.192(12)
120	0.077(15)	0.058(14)	0.138(17)	0.167(16)	0.187(12)
130	0.083(12)	0.058(12)	0.144(18)	0.173(14)	0.178(12)

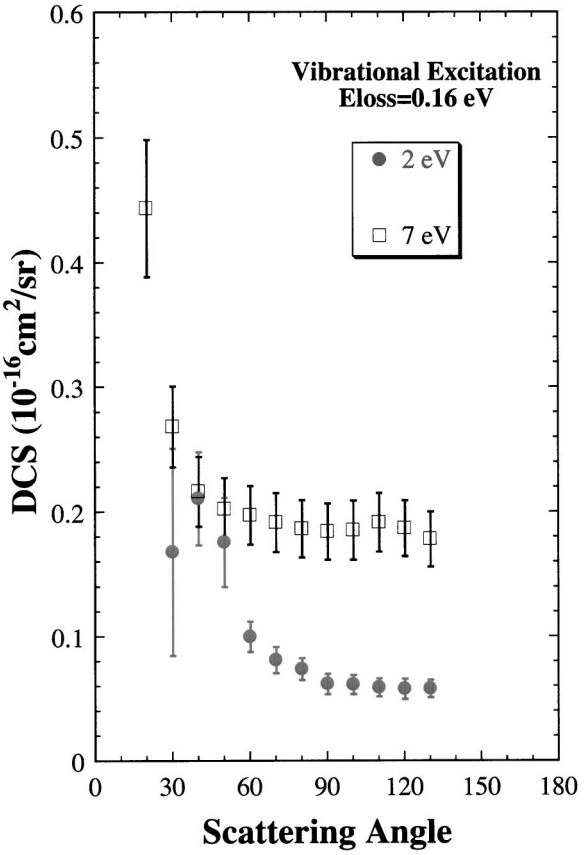

FIG. 6. Absolute differential cross sections for vibrational excitation of C_4F_8 (in units of $10^{-16}\,cm^2\,sr^{-1}$) at (●) 2 eV, (○) 7 eV.

presented in Fig. 5. Because of limited resolution of the spectrometer (50 meV) many of the low energy fundamental modes would not be resolved from the elastic peak, and the higher energy modes and their overtones, produce broad peaks at ~160 meV and possibly at ~350 meV energy loss. The former is most likely due to strong lines, which have been observed in the ir spectrum at ~120 and ~157 meV.[27]

Differential cross sections for vibrational excitation of C_4F_8, at an energy loss of 0.16 eV (the dominant loss peak) and a number of incident energies are given in Table II and two examples, at 2 and 7 eV, are shown in Fig. 6. There is little variation in the general shape of the DCS for energies between 1.5 and 7 eV with the cross section showing a slight peak at forward angles while remaining relatively flat at larger scattering angles. There are no theoretical calculations with which to compare.

Perhaps of more interest to the present discussion are measurements of the energy dependence of the excitation of this feature at 0.16 eV energy loss as they provide evidence of indirect vibrational excitation of C_4F_8 through the formation of resonant states. We have performed measurements of the energy dependence of vibrational excitation in the energy range 1.5–20 eV at scattering angles of 60° (ANU) and 50° (SU) and these are presented in Fig. 7. A large peak at 7.5 eV is clearly visible in both spectra. The rise of the cross section below 3 eV and the cross section enhancements at 4.9 and 11 eV are most likely attributable to the existence of negative ion states at these energies. The large feature at 7.5 eV could be due to the presence of a number of resonances, including those of ^2E and $^2A_2$ symmetry, which are predicted at energies of 10 and 10.6, respectively, in the calculation.

A final point to make with regard to vibrational excitation is that the energy dependence exhibited in the differential cross section in Fig. 7 is substantially different than that used for the model integral vibrational cross section of Font *et al.* They assumed a Born-dipole-like cross section for a model vibrational mode at an energy loss of 0.12 eV. The cross section that best suited the transport data had a maximum value of $6.7\times10^{-16}\,cm^2$ at 0.22 eV, decreasing monotonically to $\approx0.7\times10^{-16}\,cm^2$ at 5 eV. We can only estimate the ICS that would arise from our measurements. However, if one was to assume isotropic scattering at all energies (not too wild an assumption) then scaling our excitation function as shown in Fig. 7 by 4π would result in an ICS that was $\sim2.5\times10^{-16}\,cm^2$ at both 1.5 and 7 eV and it would clearly

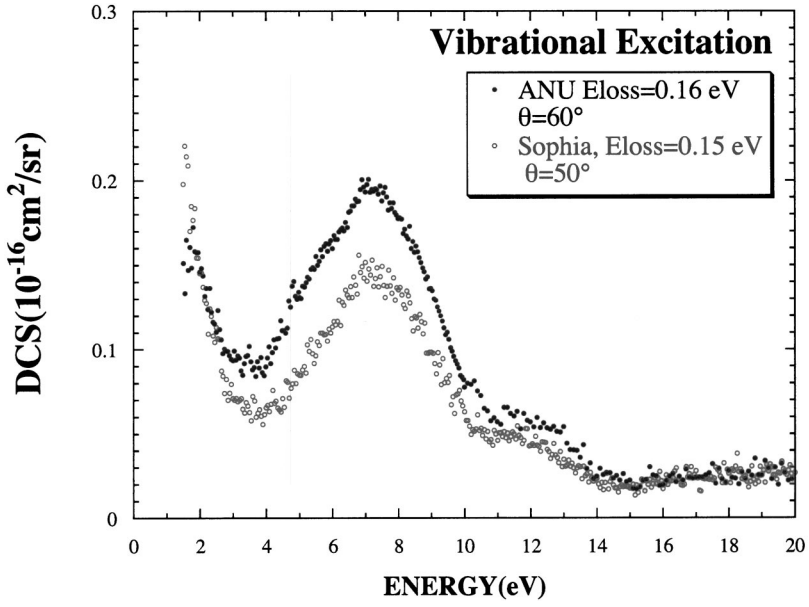

FIG. 7. The excitation function for vibrational excitation of C_4F_8 at an energy loss of 0.16 eV. The ANU data was taken at 60° scattering angle and the Sophia data at 50°.

have a substantially different energy dependence due to the presence of the many negative ion resonances.

IV. CONCLUSIONS

The present paper provides the first comprehensive set of data for elastic scattering and vibrational excitation of c-C_4F_8 by electron impact. It demonstrates the important role that resonant scattering plays in both the elastic and vibrational cross sections and provides the first real comparison test for a scattering calculation, which has previously been used as the basis for a set of cross sections for this important plasma processing gas. This calculation, which uses the Schwinger variational approach, provides an excellent description of the differential elastic scattering cross sections at energies above about 10 eV. Below this energy, the lack of any treatment of polarization effects in the theory seems to limit the level of agreement with experiment, and the theoretical calculation is seen to significantly overestimate the elastic cross section in this energy region. However, despite this limitation, the calculated cross section also gives a reasonable description of the energy dependence of the elastic cross section and provides a basis on which tentative assignments of resonant structures, observed in both elastic scattering and vibrational excitation, may be made. Hopefully the present absolute cross section measurements, together with similar recent measurements from our laboratories on C_2F_4,[28] can provide a basis for the reassessment of the accepted cross section set for c-C_4F_8 for the modeling of processing plasma discharges.

[1] K. Sasaki, Y. Kawai, C. Suzuki, and K. Kadota, J. Appl. Phys. **83**, 7482 (1998).
[2] R. A. Morris, T. M. Miller, A. A. Viggiano, and J. F. Paulson, J. Geophys. Res., [Atmos.] **100**, 1287 (1995).
[3] L. G. Christophorou and J. K. Olthoff, J. Phys. Chem. Ref. Data **30**, 449 (2001).
[4] I. Ishii, R. Mclaren, P. Hitchcock, K. D. Jordan, Y. Choi, and M. B. Robin, Can. J. Chem. **66**, 2104 (1988).
[5] T. M. Miller, R. A. Morris, A. E. S. Miller, A. A. Viaggiano, and J. F. Paulson, Int. J. Mass Spectrom. Ion Processes **135**, 195 (1994); T. M. Miller, J. F. Friedman, and A. A. Viggiano, J. Chem. Phys. **120**, 7024 (2204).
[6] J. E. Sanabia, G. D. Cooper, J. A. Tossell, and J. H. Moore, J. Chem. Phys. **108**, 389 (1998).
[7] H. Nishimura, *Proceedings of the International Symposium on Electron-Molecule Collisions and Swarms*, Tokyo, Japan 18–20 July, 1999, edited by Y. Hatano, H. Tanaka, and N. Kouchi, p. 103.
[8] M. V. Kurepa, third Cz. Conference on Electronics and Vacuum Physics Transactions, 1965.
[9] S. M. Spyrou, S. R. Hunter, and L. G. Christophorou, J. Chem. Phys. **72**, 4223 (1980).
[10] A. Chutjian and S. H. Alajajian, J. Phys. B **20**, 839 (1987).
[11] J. P. Novak and M. F. Frechette, J. Appl. Phys. **63**, 2570 (1988).
[12] M. S. Naidu, A. N. Prasad, and J. D. Craggs, J. Phys. D **5**, 741 (1972).
[13] M. Yamaji, Y. Okadam, and Y. Nakamura, In *Proceedings of the International Symposium on Electron-Molecule Collisions and Swarms*, Tokyo, Japan 18–20 July (1999), edited by Y. Hatano, H. Tanaka, and N. Kouchi.
[14] H. Toyoda, M. Ito, and H. Sugai, Jpn. J. Appl. Phys., Part 1 **36**, 3730 (1997).
[15] C. Q. Jiao, A. Garscadden, and P. D. Haaland, Chem. Phys. Lett. **297**, 121 (1998).
[16] G. I. Font, W. L. Morgan, and G. Mennenga, J. Appl. Phys. **91**, 3530 (2002).
[17] C. Winstead and V. McKoy, J. Chem. Phys. **114**, 7407 (2001).
[18] M. J. Brunger, S. J. Buckman, D. S. Newman, and D. T. Alle, J. Phys. B **24**, 1435 (1991).
[19] H. Tanaka, L. Boesten, D. Matsunga, and T. Kudo, J. Phys. B **21**, 1255 (1988).
[20] M. Kitajima, Y. Sakamoto, R. J. Gulley, M. Hoshino, J. C. Gibson, H. Tanaka, and S. J. Buckman, J. Phys. B **33**, 1687 (2000).
[21] M. A. Khakoo and S. Trajmar, Phys. Rev. A **34**, 138 (1986).
[22] M. J. Brunger and S. J. Buckman, Phys. Rep. **357**, 215 (2002).
[23] R. K. Nesbet, Phys. Rev. A **20**, 58 (1979).
[24] L. Boesten and H. Tanaka, At. Data Nucl. Data Tables **52**, 25 (1992).
[25] D. Fursa and I. Bray, J. Phys. B **30**, 757 (1997).
[26] R. Panajotovic, M. Kitajima, H. Tanaka, M. Jelisavcic, J. Lower, L. Campbell, M. J. Brunger, and S. J. Buckman, J. Phys. B **36**, 1615 (2003).
[27] C. Winstead (private communication).
[28] R. Panajotovic, M. Jelisavcic, R. Kajita, T. Tanaka, M. Kitajima, H. Cho, H. Tanaka, and S. J. Buckman, J. Chem. Phys. **121**, 4559 (2004).